AJNR

MR Imaging of Partially Thrombosed Cerebral Aneurysms: Characteristics and Evolution

A.J. Martin, S.W. Hetts, W.P. Dillon, R.T. Higashida, V. Halbach, C.F. Dowd, M.T. Lawton and D. Saloner

A.J. Martin
S.W. Hetts
W.P. Dillon
R.T. Higashida
V. Halbach
C.F. Dowd
M.T. Lawton
D. Saloner

MR Imaging of Partially Thrombosed Cerebral Aneurysms: Characteristics and Evolution

BACKGROUND AND PURPOSE: A comprehensive evaluation of aneurysmal morphometry requires appreciation of both the vascular lumen and the intraluminal thrombus. MR imaging methods can both evaluate the lumen and directly image the vessel wall. We investigated the ability of T1-weighted, T2-weighted, and steady-state MR imaging techniques to delineate thrombus morphology and reveal changes with time.

MATERIALS AND METHODS: Nine patients with fusiform basilar or intracranial vertebral artery aneurysms that contained intraluminal thrombus were studied with MR imaging. All patients underwent at least 2 imaging sessions, which were separated by 4–22 months. Analysis of signal intensity to determine the mean signal intensity from thrombus, blood, CSF, and brain in matched regions was performed. Aneurysm maximal diameter and cross-sectional area were determined with and without thrombus.

RESULTS: Thrombus was identified on all image sequences, and its general appearance was consistent between imaging sessions. Thrombus produced the highest and most consistent signal intensities with T1-weighted and steady-state techniques, though the latter showed superior contrast between luminal blood and thrombus. Heterogeneity within clot was evident in 4/9 of patients, with peripheral hyperintensity being a common feature.

CONCLUSIONS: Steady-state imaging was found to be superior to T1- and T2-weighted imaging for delineating and characterizing intraluminal thrombus within aneurysms. The imaging characteristics of intraluminal thrombus proved to be very consistent for long periods. Assessment of overall aneurysm size, including thrombosed portions, permits more accurate evaluation of aneurysm growth and concomitantly may permit more informed clinical decision-making with regard to the timing and need for aneurysm treatment.

ABBREVIATIONS: BW = bandwidth; CE-MRA = contrast-enhanced MR angiography; MIP = maximum intensity projection; SENSE = sensitivity encoding; SSFP = steady-state free precession

U nruptured intracranial aneurysms are detected in approximately 2% of patients who undergo MR angiography[1,2]; the overall prevalence of unruptured intracranial aneurysm is estimated to be approximately 1% of the population.[3,4] Aneurysm treatments, including surgical clipping or endovascular coiling, are typically advocated when the risk of rupture is considered to exceed the therapeutic risks. Factors thought to affect aneurysm progression and risk of rupture include aneurysm size,[5,6] location,[7] and morphometry.[8] Increasingly, factors such as hemodynamics[9] and the perianeurysmal environment[10] are also being recognized as possible contributors to aneurysm growth and evolution. Aneurysms, however, are typically detected and monitored with angiographic techniques that interrogate lumen morphology and provide little

insight into extraluminal anatomy. A comprehensive evaluation of aneurysm morphometry requires appreciation of both the vascular lumen and extraluminal anatomy and pathology. The delineation and characterization of intraluminal thrombus specifically may be highly relevant to understanding disease progression and risk of rupture or emboli. Furthermore, an improved understanding of the impact of mass effect from aneurysms (particularly fusiform posterior circulation aneurysms) requires a detailed depiction of the outer wall of the aneurysm.

MR imaging methods are capable of both angiographic evaluation and direct imaging of the vessel wall. MR angiographic methods can be based on inflow properties, blood velocities, or contrast enhancement. Aneurysms, which may have regions of relatively slowly recirculating flow, can be poorly visualized with MR angiographic techniques that rely on inflow or blood velocity (eg, time-of-flight and phase-contrast methods). CE-MRA does not have these limitations and has been demonstrated to provide superior depiction of the vascular lumen in aneurysm models.[11] MR imaging techniques are capable of visualizing thrombus and may provide insight into thrombus age.[12] To our knowledge, the characteristics and evolution of clot within partially thrombosed neurovascular aneurysms, however, have not been well defined.

We investigated neurovascular aneurysm morphology with a combination of CE-MRA for defining the vascular lumen and an assortment of MR imaging techniques for characterizing anatomy external to the free lumen. We specifically
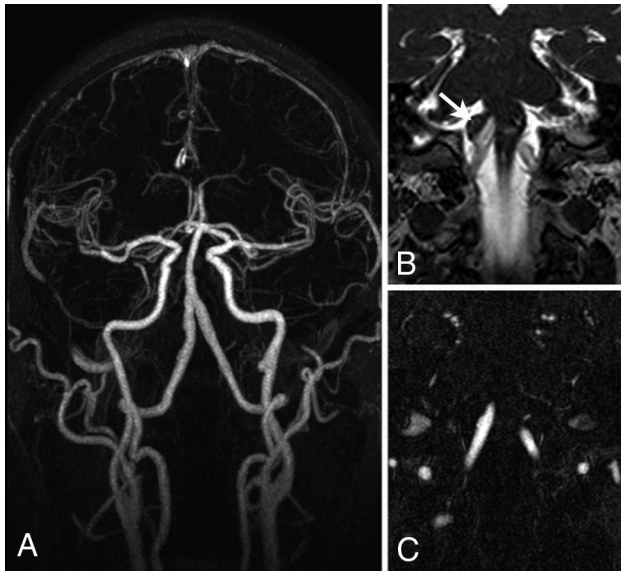
Fig 1. *A*, MIP of a contrast-enhanced angiogram of a right vertebral artery aneurysm. *B* and *C*, Matched sections from the SSFP image (*B*) and the angiogram (*C*) reveal a thrombosed component to the aneurysm (*arrow* in *B*), which indicates a substantially larger aneurysm than can be appreciated on the angiogram alone.

assessed the ability of T1-weighted, T2-weighted, and steady-state MR imaging techniques to delineate intraluminal thrombus and to reveal heterogeneity within the clot. Aneurysm and clot morphology were studied during relatively long time intervals to characterize the evolution of intraluminal thrombus.

Materials and Methods

Patients

Patients in this study were selected from a larger cohort of patients with intracranial aneurysms who are being studied at our institution. These patients are being followed with MR imaging as part of a study of the natural history of the evolution of cerebral aneurysms. Of the 85 patients in the full cohort, 9 (7 men, 2 women) with a history of unruptured and untreated fusiform basilar or intracranial vertebral artery aneurysms who were also noted to have intraluminal thrombus at ≥2 time points were included in this evaluation. A diagnosis of intraluminal thrombus was based on a nonenhancing MR imaging–visible mass within the aneurysmal portion of the affected artery. All studies were performed with the approval of the committee for human research of our institution, and all patients provided written informed consent. Average patient age was 65 years (range = 43–79 years) at the time of the first study, and all patients underwent multiple MR imaging studies, which were separated by a minimum of 4 months.

Imaging

Imaging was performed on a 1.5T MR imaging system (Achieva; Philips Healthcare, Cleveland, Ohio) with either a 6-channel head coil or a 16-channel head/neck coil. Imaging included contrast-enhanced angiography (3D spoiled gradient-echo: FOV = 240 × 180 × 54 mm, matrix = 400 × 286 × 45, TR/TE = 5.0/1.8 ms, flip angle = 30°, SENSE factor = 2, BW = 302 Hz/pixel, scanning time = 34 seconds) to reveal the free lumen and T1-weighted (2D turbo spin-echo: FOV = 220 × 177, matrix = 304 × 244, section = 2 mm, number of sections = 24, TR/TE = 400/14 ms, flip angle = 90°, turbo factor = 3,

BW = 263 Hz/pixel, NEX = 3, scanning time = 3 minutes 18 seconds), T2-weighted (3D turbo spin-echo: FOV = 240 × 180 × 54 mm, matrix = 256 × 166 × 45, TR/TE = 1500/120 ms, flip angle = 90°, turbo factor = 57, SENSE factor = 2, BW = 304 Hz/pixel, NEX = 1, scanning time = 2 minutes 3 seconds), and steady-state or balanced fast-field echo (SSFP: FOV = 240 × 180 × 54 mm, matrix = 256 × 176 × 45, TR/TE = 4.9/1.7 ms, flip angle = 60°, BW = 302 Hz/pixel, NEX = 3, scanning time = 1 minute 57 seconds) sequences for imaging the vascular lumen as well as intraluminal thrombus (full lumen) and extraluminal anatomy. The CE-MRA scan was oriented in an oblique coronal slab that encompassed the full aneurysm, vertebral and basilar arteries, and, usually, the full course of both carotid arteries. MR imaging was performed either in an axial plane centered on the aneurysm or in an oblique coronal plane matching the CE-MRA sequence.

Image Analysis

The maximum free lumen diameter of the aneurysm was measured from the CE-MRA data for each study. MIPs were created of the vessel segment and rotated around the principal axis of the vessel in 6° increments. The MIP view revealing the largest free lumen diameter was selected, and a manual measurement of maximal diameter was established. The cross-sectional area of the free lumen of the aneurysm at this level was obtained by reformatting the CE-MRA data into oblique axial planes that were perpendicular to the principal axis of the artery segment. The cross-sectional area of the lumen at this level was defined by manually drawing a region that conformed to the vessel edge, with the scanner software. The area of this region of interest was taken as the free lumen cross-sectional area. SSFP imaging data were used to define the maximal full lumen, including intraluminal thrombus, diameter, and cross-sectional area. Oblique axial reformats of the SSFP images were generated in which the aneurysmal vessel segment ran approximately perpendicular to the image plane. The data were manually inspected to find the level at which the full lumen diameter was maximal. The maximal diameter and cross-sectional area of the aneurysm were then extracted in a manner analogous to the free-lumen measurements.

Signal-intensity analysis was performed to characterize the relative signal intensity of thrombus, blood, and CSF on the various imaging sequences. Regions of interest were established within each of these tissue types, and the mean signal intensity was normalized to the signal intensity of normal brain in the respective imaging sequence. Means and SDs of signal intensity were established for each region of interest. The spatial coordinates of the regions of interest were matched between imaging sequences to assure that they corresponded to identical anatomic regions. Signal intensity from flowing blood was averaged over the central portion of the free lumen, while representative regions within intraluminal thrombus were selected. CSF regions of interest were placed near the aneurysmal segment of the artery, and this signal intensity was monitored as a control for the consistency of the signal-intensity levels. Region-of-interest placement in patients who returned for subsequent evaluation was performed by manually placing the regions of interest in regions that were consistent with previously acquired data.

Results

Partially thrombosed fusiform aneurysms of the basilar (n = 8) or intracranial vertebral (n = 1) arteries were present in all subjects. All patients were on oral antithrombotic agents (aspirin, combination aspirin/extended-release dipyridamole, or
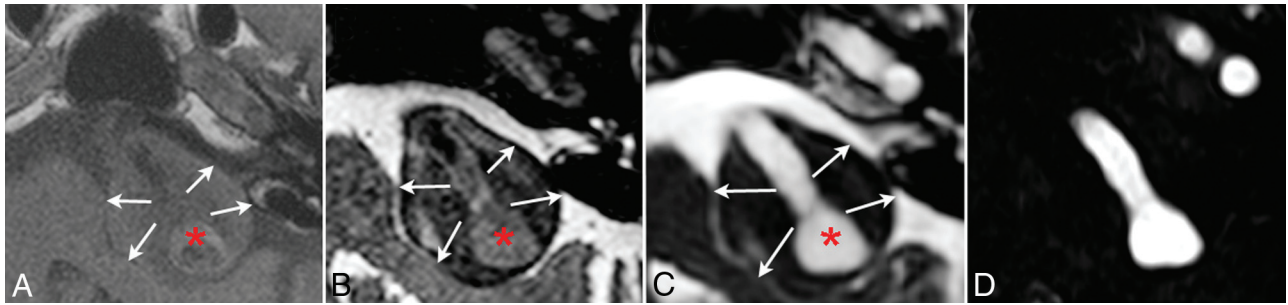
Fig 2. The relative image contrast achieved with T1-weighted (*A*), T2-weighted (*B*), and SSFP (*C*) images are shown for this partially thrombosed basilar aneurysm. A matched section from the CE-MRA (*D*) reveals the free lumen (*asterisks in A–C*) and the thrombosed region (*arrows in A–C*).

Table 1: Signal-intensity analysis of aneurysm thrombus: signal intensities normalized to brain[a]

Tissue	T1-Weighted	T2-Weighted	Steady-State
Thrombus core	1.1 ± 0.3	0.6 ± 0.3	1.1 ± 0.3
Thrombus rim	1.5 ± 0.2	0.6 ± 0.2	2.3 ± 0.3
Blood	1.0 ± 0.3	1.4 ± 0.8	4.3 ± 1.7
CSF	0.5 ± 0.1	3.6 ± 0.2	7.2 ± 0.9

[a] Thrombus heterogeneity with a rim evident occurred in 4/9 subjects.

warfarin) and underwent multiple MR imaging studies with an average time between studies of 10.3 months (range = 4–22 months). Four patients were studied 3 times, and 5 patients underwent 2 MR imaging examinations in which thrombus was evident. Two patients initially presented with basilar aneurysms without intraluminal thrombus but developed thrombus during serial monitoring. Only studies that demonstrated a partially thrombosed aneurysm were considered for this analysis.

Thrombus was detected in 2 individuals in whom angiographic evaluations provided only subtle evidence of aneurysmal disease (Fig 1). In other patients, aneurysm size and volume were substantially larger when intraluminal thrombus was considered. The On-line Table summarizes the maximal arterial diameter and axial cross-sectional area of all aneurysms when considering only the free lumen and when including intraluminal thrombus (full lumen). These parameters were tracked over multiple studies, and it was found that whereas the maximal cross-sectional area of the free lumen decreased on average ($-6.3 \pm 13.5\%$), the maximal cross-sectional area of the full lumen increased on average ($+4.1 \pm 9.5\%$). The increase in maximal aneurysm diameter was similarly more dramatic when including thrombus ($+9.1 \pm 8.7\%$) than when considering only the free lumen ($+2.8 \pm 6.4\%$). These findings indicate that serial monitoring of aneurysms without evaluating intraluminal thrombus could lead to erroneous or misleading results.

The appearance (Fig 2) and signal-intensity properties of various tissue types on T1-weighted, T2-weighted, and steady-state imaging are summarized in Table 1. The signal intensity of brain, in a region devoid of CSF, was used to normalize signal intensity. The mean and range of region-of-interest sizes for the various tissue types were as follows: blood = 22 mm^2 (range = 6.7–38.6 mm^2), thrombus core = 54.4 mm^2 (range = 11.8–129.4 mm^2), thrombus rim = 11.5 mm^2 (range = 6.0–14.8 mm^2), CSF = 28 mm^2 (range = 18.5–45.8 mm^2), and brain = 56.8 mm^2 (range = 32.7–78.8 mm^2). The

ratio of normalized signal intensities of different tissues was relatively consistent among subjects for all imaging protocols. Blood signal intensity provided the highest degree of variability with all acquisition types, presumably due to flow effects. Thrombus signal intensity was homogeneous in 5 patients and heterogeneous in 4 patients. Heterogeneous thrombus exhibited peripheral hyperintenisty toward the arterial wall side of the thrombus, and signal intensity was, therefore, separated into 2 zones, core and rim. Only those patients with a heterogeneous appearance were subjected to the thrombus rim signal-intensity evaluation.

Regions of interest were manually placed in matched regions for each image contrast (Fig 3*A*–*C*), and representative signal intensities were established across all patients. MR imaging signal intensity within the core of the thrombus was highest on T1-weighted and steady-state imaging and lowest with T2-weighted imaging. Thrombus produced signal intensities that were comparable with brain with T1 and steady-state techniques and generally lower than brain with T2 techniques (Figs 2 and 3). Heterogeneity within the clot was evident on T1-weighted and steady-state images in 4/9 patients, with peripheral hyperintensity being a consistent feature. Peripheral hyperintensity on these sequences was consistent, with T1-shortening being the primary source of thrombus contrast. Contrast (ie, ratio of mean signal intensities) between luminal blood and thrombus was greatest with steady-state techniques (3.9), followed by T2-weighted (2.3) and T1-weighted (0.9) imaging. Contrast between thrombus and surrounding CSF was similarly greatest with steady-state techniques (6.5), followed closely by T2-weighted (6.0) imaging.

The characteristics of intraluminal thrombus were evaluated with time. Visually, the thrombus remained remarkably consistent in appearance between imaging sessions (Fig 3*C*, *-D*). This consistency was corroborated by signal-intensity analysis (Table 2), which implies that mature intraluminal thrombus is either relatively static or in some form of equilibrium. These findings included heterogeneous thrombus, which maintained a relatively consistent pattern of peripheral hyperintensity on T1-sensitive imaging. Thrombus hyperintensity along the arterial wall may indicate involvement of the vasa vasorum. Indeed, evidence of delayed enhancement of the arterial wall on T1-weighted images performed immediately following the contrast-enhanced angiogram showed hyperintensity external to the thrombus and within the arterial wall (Fig 4). In contrast, there was little evidence of thrombus
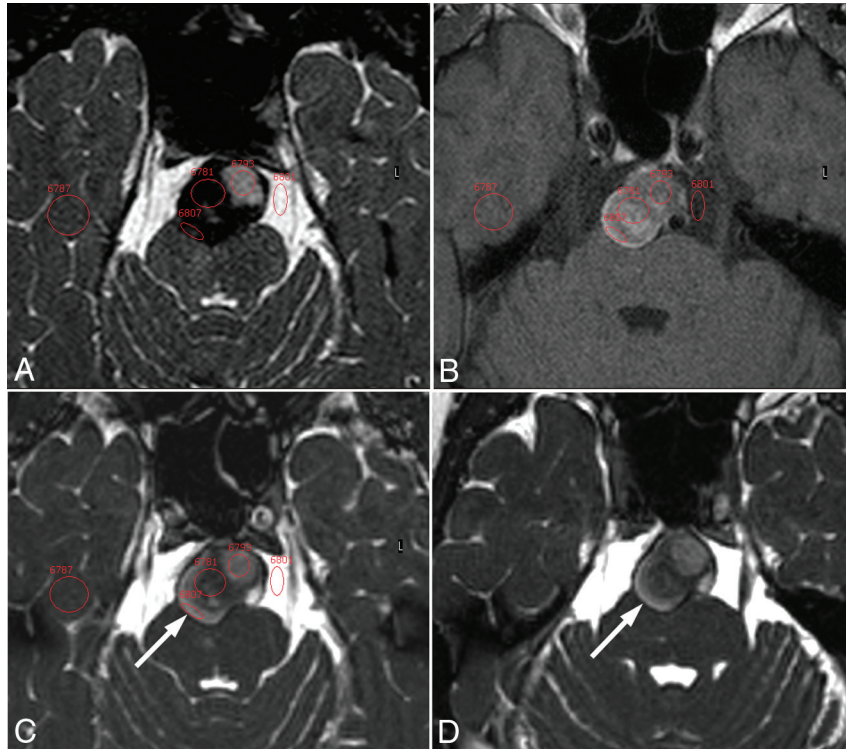
Fig 3. This summary array shows examples of the matched regions of interest that were used to establish relative signal intensities of thrombus core and rim, blood, CSF, and brain on T2-weighted (*A*), T1-weighted (*B*), and SSFP (*C*) images. Signal intensities were normalized to those of brain in a region devoid of CSF based on the SSFP and T2-weighted images. The evolution of thrombus during a 1-year interval is also demonstrated in SSFP images (*C* and *D*). Both images are at the same level of the aneurysm, though there is a slight difference in the obliquity of the axial plane. The hyperintense outer rim of the thrombosed region of the aneurysm (*arrows*) is evident in both studies, and the general contrast properties of the thrombus remain remarkably consistent during this interval.

Table 2: Evolution of thrombus SSFP signal intensities with time[a]

Study	Thrombus Core	Thrombus Rim	Blood	CSF
Baseline	1.1 ± 0.3	2.3 ± 0.3	4.3 ± 1.7	7.2 ± 0.9
Follow-up	1.0 ± 0.1	2.2 ± 0.7	4.3 ± 2.6	7.2 ± 1.4

[a] Thrombus heterogeneity with a rim evident occurred in 4/9 subjects.

heterogeneity toward the luminal surface and no evidence of delayed enhancement of this surface following contrast administration.

Discussion

In this study, we evaluated the ability of different MR imaging protocols to detect and characterize intraluminal thrombus within aneurysms. However, we were not able to definitively establish that the intraluminal structure we were observing was, in fact, thrombus. The diagnosis of intraluminal thrombus was based on the presence of a nonenhancing intraluminal mass within an aneurysmal artery segment, as defined by a convex outer border of the vessel. Thrombus could be distinguished from atheroma, which exhibits a relatively linear or only moderately outwardly remodeled outer surface, based largely on these geometric considerations. Furthermore, we did not observe many of the other features that are generally present in atherosclerotic plaque,[13] such as a fibrous cap overlying a necrotic core, the presence of large calcified regions, or the presence of luminal surface irregularity or frank ulceration. In 2 instances, we were also able to demonstrate that thrombus

formation occurred relatively quickly due to serial monitoring that initially did not indicate the presence of this structure. Thus, while we cannot definitively establish that the observed intraluminal mass was truly thrombus, we have a high degree of confidence in this diagnostic evaluation.

The presence of thrombus may have a strong impact on the risk associated with an aneurysm and the manner in which it is likely to evolve. It has already been established for abdominal aortic aneurysms that a substantial clot burden is associated with higher aneurysm growth rates.[14] Fusiform intracranial aneurysms are challenging to manage clinically.[15-17] Watchful waiting exposes the patient to continued risk of aneurysm rupture, progressive mass effect on critical neural structures, local thrombosis causing small perforating artery infarcts, or distal embolization of thrombus causing large-vessel infarction. Patients are often placed on antiplatelet or anticoagulant agents to reduce the risk of local thrombosis or distal embolization, though such agents may increase the extent of hemorrhage if an aneurysm ruptures. Surgical intracranial arterial bypass procedures, selective arterial clipping, clip reconstruction, bypass/trapping, endovascular covered stent placement or flow diversion, and endovascular coil occlusion of fusiform aneurysms or their input arteries have all been used with variable success to reduce flow to fusiform aneurysms while maintaining perfusion of brain stem perforating arteries.[18-23] The ability to accurately detect, delineate, and characterize aneurysm thrombus noninvasively, therefore, may
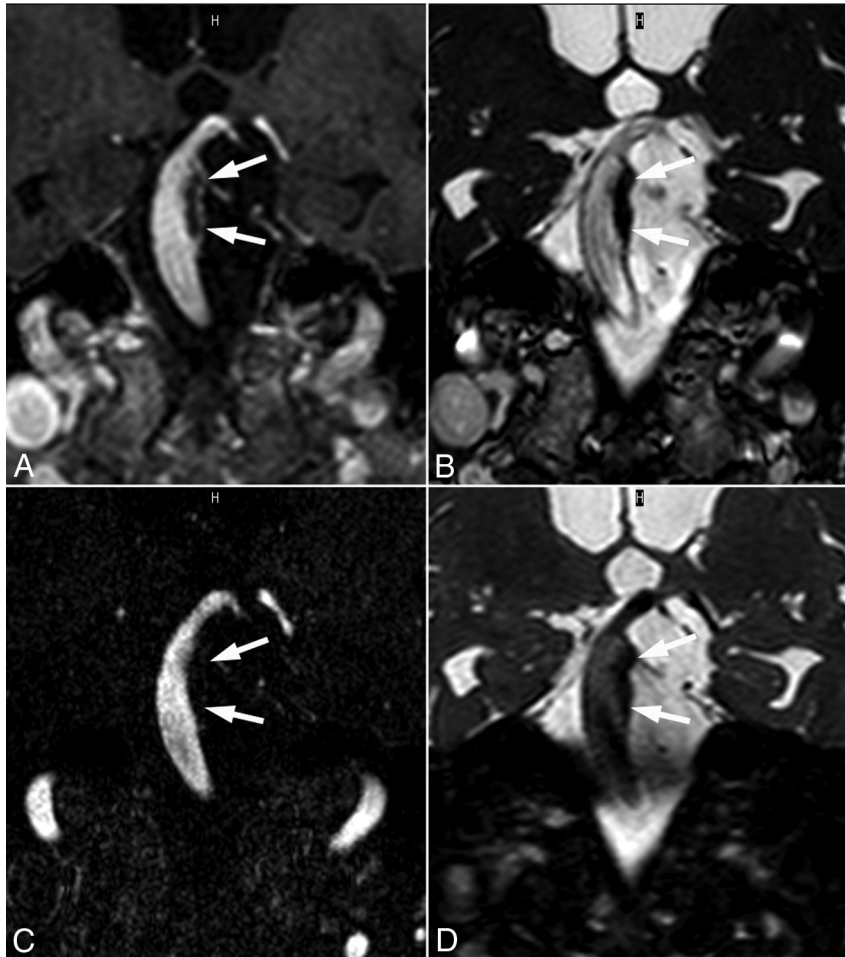
Fig 4. This partially thrombosed (*arrows*) basilar aneurysm is demonstrated on postcontrast T1-weighted (*A*), SSFP (*B*), CE-MRA (*C*), and T2-weighted (*D*) images. These matched oblique coronal scanning planes reveal the extent of thrombosis and further indicate delayed enhancement of the arterial wall underlying the thrombosis (*A*).

have significant clinical relevance in the management of patients with challenging fusiform aneurysms.

SSFP techniques were found to offer several advantages over either T1-weighted or T2-weighted imaging for detecting and characterizing thrombus: They provide moderate signal intensity-to-noise ratio within thrombus, exhibit signal-intensity heterogeneity within thrombus that is similar to that of T1-weighted imaging, and provide contrast against the blood pool and surrounding CSF that is comparable with or superior to that of T2-weighted imaging. Collectively, these data support the hypothesis that SSFP is the superior method for delineating and characterizing intraluminal thrombus. SSFP imaging has been widely developed for numerous applications, including cardiac imaging, angiography, and other pseudo-T2-weighted applications.[24] SSFP offers high inherent signal intensity-to-noise ratio, exhibits contrast that is proportional to the square root of the ratio of T2 to T1, and is relatively motion-insensitive. Intraluminal thrombus was found to be either homogeneous in appearance on MR images or heterogeneous with a characteristic peripheral rim hyperintensity on T1-sensitive images. The presence of hyperintensity toward the arterial wall, rather than the arterial lumen, was somewhat unexpected. While there has been little attention in the literature, an early MR imaging study reported the opposite effect, with hyperintensity toward the luminal surface.[25] This report,

however, focused on acute findings in 2 patients who were being evaluated for immediate intervention. Conversely, our study analyzed patients with clinically stable conditions who exhibited intra-aneurysmal thrombus chronically. A more recent study of the growth potential of partially thrombosed aneurysms of the posterior circulation[26] revealed findings similar to those reported here, albeit only with postcontrast T1-weighted imaging. Another study of incidentally discovered vertebrobasilar fusiform aneurysms[27] also showed evidence of peripheral T1-related hyperintensity, though the authors were unsure whether this indicated the presence of thrombus or was a flow effect.

The signal intensity within both the core and periphery of the thrombus was found to be relatively constant for long periods of a year or more. This implies that the thrombus is either stagnant or in some form of dynamic equilibrium. In general, areas where there has been a fresh bleed will appear as hyperintense on T1-weighted imaging, denoting the presence of methemoglobin, a transformation product of oxyhemoglobin that is thought to transiently appear as thrombus ages.[12] In the aneurysm studies here, the presence and retention of T1 shortening toward the arterial wall suggests that relatively fresh thrombus may exist at this location. If this is the case, then it could be hypothesized that thrombus is continually being deposited on the arterial wall side of the thrombus and may be shedding from the luminal surface.

Postcontrast enhancement of the arterial wall side of the thrombus provides additional support for this hypothesis. Thus, it is possible that thrombi that present with a hyperintense rim and whose appearance remains constant under MR imaging may, in fact, be undergoing continuous remodeling. However, this has not been established histologically and thus represents a limitation of the study.

We evaluated conventional measures of aneurysm size, including maximal diameter and cross-sectional area, and studied the extent to which the inclusion of the thrombosed region affected the reported values. We further studied these parameters with time to determine the extent to which they evolved. When thrombus is present, the free lumen diameter and cross-sectional area may well decrease or remain unchanged while the true aneurysm diameter and cross-sectional area continue to grow. Thus, the inclusion of intraluminal thrombus is important to accurately stage the geometric properties of an aneurysm and may provide insights into the risk of rupture or symptomatic progressive enlargement of thrombosis with time. Thrombus deposition and aneurysm morphometry, however, are inherently 3D, and a comprehensive evaluation of aneurysm geometric properties and how they evolve with time requires more sophisticated analysis.[28] While this may not be possible at many centers, it is clearly important to include the thrombosed component in any measures that are made. This represents an additional advantage of steady-state techniques, which are fast and readily adapted to 3D volumetric coverage.

Conclusions

Steady-state MR imaging was found to be superior to T1- and T2-weighted imaging for delineating and characterizing intraluminal thrombus within aneurysms. The general characteristics of intraluminal thrombus were found to be remarkably consistent with time, and a common feature was a hyperintense peripheral rim on T1-sensitive imaging. It is further demonstrated that measures of maximal arterial diameter or cross-sectional area that do not include intraluminal thrombus can provide erroneous or misleading findings about aneurysm progression. A complete evaluation of aneurysm morphometry, including thrombosed portions, is necessary when making clinical decisions regarding the necessity and timing of possible aneurysm treatment.

References

1. Horikoshi T, Akiyama I, Yamagata Z, et al. **Retrospective analysis of the prevalence of asymptomatic cerebral aneurysm in 4518 patients undergoing magnetic resonance angiography: when does cerebral aneurysm develop?** *Neurol Med Chir (Tokyo)* 2002;42:105–12, discussion 113
2. Matsumoto E, Shinoda S, Masuzawa T, et al. **Observation of statistics of screening for unruptured cerebral aneurysms in Tochigi prefecture** [in Japanese]. *No Shinkei Geka* 2002;30:829–36
3. Inagawa T, Hirano A. **Autopsy study of unruptured incidental intracranial aneurysms.** *Surg Neurol* 1990;34:361–65
4. Rinkel GJ, Djibuti M, Algra A, et al. **Prevalence and risk of rupture of intracranial aneurysms: a systematic review.** *Stroke* 1998;29:251–56
5. **Unruptured intracranial aneurysms: risk of rupture and risks of surgical intervention—International Study of Unruptured Intracranial Aneurysms Investigators.** *N Engl J Med* 1998;339:1725–33
6. Wiebers DO, Whisnant JP, Huston J 3rd, et al. **Unruptured intracranial aneurysms: natural history, clinical outcome, and risks of surgical and endovascular treatment.** *Lancet* 2003;362:103–10
7. Weir B, Disney L, Karrison T. **Sizes of ruptured and unruptured aneurysms in relation to their sites and the ages of patients.** *J Neurosurg* 2002;96:64–70
8. Hademenos GJ, Massoud TF, Turjman F, et al. **Anatomical and morphological factors correlating with rupture of intracranial aneurysms in patients referred for endovascular treatment.** *Neuroradiology* 1998;40:755–60
9. Cebral JR, Castro MA, Burgess JE, et al. **Characterization of cerebral aneurysms for assessing risk of rupture by using patient-specific computational hemodynamics models.** *AJNR Am J Neuroradiol* 2005;26:2550–59
10. Satoh T, Omi M, Ohsako C, et al. **Influence of perianeurysmal environment on the deformation and bleb formation of the unruptured cerebral aneurysm: assessment with fusion imaging of 3D MR cisternography and 3D MR angiography.** *AJNR Am J Neuroradiol* 2005;26:2010–18
11. Isoda H, Takehara Y, Isogai S, et al. **MRA of intracranial aneurysm models: a comparison of contrast-enhanced three-dimensional MRA with time-of-flight MRA.** *J Comput Assist Tomogr* 2000;24:308–15
12. Corti R, Osende JI, Fayad ZA, et al. **In vivo noninvasive detection and age definition of arterial thrombus by MRI.** *J Am Coll Cardiol* 2002;39:1366–73
13. Yuan C, Kerwin WS. **MRI of atherosclerosis.** *J Magn Reson Imaging* 2004;19:710–19
14. Speelman L, Schurink GW, Bosboom EM, et al. **The mechanical role of thrombus on the growth rate of an abdominal aortic aneurysm.** *J Vasc Surg* 2010;51:19–26
15. Hetts SW, Narvid J, Sanai N, et al. **Intracranial aneurysms in childhood: 27-year single-institution experience.** *AJNR Am J Neuroradiol* 2009;30:1315–24
16. Wakhloo AK, Mandell J, Gounis MJ, et al. **Stent-assisted reconstructive endovascular repair of cranial fusiform atherosclerotic and dissecting aneurysms: long-term clinical and angiographic follow-up.** *Stroke* 2008;39:3288–96
17. Gonzalez NR, Duckwiler G, Jahan R, et al. **Challenges in the endovascular treatment of giant intracranial aneurysms.** *Neurosurgery* 2008;62(6 suppl 3):1324–35
18. Lubicz B, Collignon L, Lefranc F, et al. **Circumferential and fusiform intracranial aneurysms: reconstructive endovascular treatment with self-expandable stents.** *Neuroradiology* 2008;50:499–507
19. Greenberg E, Katz JM, Janardhan V, et al. **Treatment of a giant vertebrobasilar artery aneurysm using stent grafts: case report.** *J Neurosurg* 2007;107:165–68
20. Drake CG, Peerless SJ. **Giant fusiform intracranial aneurysms: review of 120 patients treated surgically from 1965 to 1992.** *J Neurosurg* 1997;87:141–62
21. Ferns SP, van Rooij WJ, Sluzewski M, et al. **Partially thrombosed intracranial aneurysms presenting with mass effect: long-term clinical and imaging follow-up after endovascular treatment.** *AJNR Am J Neuroradiol* 2010;31:1197–205. Epub 2010 Mar 18
22. Szikora I, Berentei Z, Kulcsar Z, et al. **Treatment of intracranial aneurysms by functional reconstruction of the parent artery: the Budapest experience with the Pipeline embolization device.** *AJNR Am J Neuroradiol* 2010;31:1139–47
23. van Rooij WJ, Sluzewski M. **Perforator infarction after placement of a Pipeline flow-diverting stent for an unruptured A1 aneurysm.** *AJNR Am J Neuroradiol* 2010;31:E43–44. Epub 2010 Feb 11
24. Scheffler K, Lehnhardt S. **Principles and applications of balanced SSFP techniques.** *Eur Radiol* 2003;13:2409–18
25. Atlas SW, Grossman RI, Goldberg HI, et al. **Partially thrombosed giant intracranial aneurysms: correlation of MR and pathologic findings.** *Radiology* 1987;162(1 pt 1):111–14
26. Iihara K, Murao K, Yamada N, et al. **Growth potential and response to multimodality treatment of partially thrombosed large or giant aneurysms in the posterior circulation.** *Neurosurgery* 2008;63:832–42, discussion 842–44
27. Yasui T, Komiyama M, Iwai Y, et al. **Evolution of incidentally-discovered fusiform aneurysms of the vertebrobasilar arterial system: neuroimaging features suggesting progressive aneurysm growth.** *Neurol Med Chir (Tokyo)* 2001;41:523–27, discussion 528
28. Boussel L, Wintermark M, Martin A, et al. **Monitoring serial change in the lumen and outer wall of vertebrobasilar aneurysms.** *AJNR Am J Neuroradiol* 2008;29:259–64